Proceedings of the ASME 2013 International Design Engineering Technical Conferences & Mechanisms and Robotics Conference
IDETC/MECH 2013
August 4-7, 2013, Portland, Oregon, USA

DETC2013-12799

DIMENSIONAL SYNTHESIS OF PLANAR EIGHT-BAR LINKAGES BASED ON A PARALLEL ROBOT WITH A PRISMATIC BASE JOINT

Gim Song Soh
Engineering Product Development
Singapore University of Technology and Design
Singapore 138682
Email: sohgimsong@sutd.edu.sg

Fangtian Ying
International Design Institute
Zhejiang University
Hangzhou, Zhejiang Province, 310058
P. R. China
Email: yingft@gmail.com

ABSTRACT

This paper details the dimensional synthesis for the rigid body guidance of planar eight-bar linkages that could be driven by a prismatic joint at its base. We show how two RR cranks can be added to a planar parallel robot formed by a PRR and 3R serial chain to guide its end-effector through a set of five task poses. This procedure is useful for designers who require the choice of ground pivot locations. The results are eight different types of one-degree of freedom planar eight-bar linkages. We demonstrate the design process with the design of a multifunctional wheelchair that could transform its structure between a self-propelled wheelchair and a walking guide.

INTRODUCTION

This paper focuses on the dimensional synthesis for the rigid body guidance of planar eight-bar linkages with 8 links and 10 joints, of which one of the joint is a sliding joint located at the base. Design situations frequently arise where actuating a mechanism with a prismatic joint offers significant advantage, particularly if it involves large driving forces and repeatable positional accuracy, see Myszka and Murray (2010) [1]. Alternatively, it would be useful in circumstances where huge output forces are required, for instance to deliver a linear projectile to "render-safe" ordnance, see Gazonas etal. (1996) [2].

Dimensional synthesis determines the dimensions or proportions of the links of a linkage, and in rigid body guidance we require the linkage to guide an entire body through a prescribed motion sequence. A planar linkage is made up of revolute (R) and prismatic (P) joints and has the property that all of its links move in parallel planes. An example of a well known planar eight-bar linkage is the Peaucellier linkage, invented by the French Captain Charles Nicolas Peaucellier, which is able to follow a straight line exactly, see Koetsier (1994) [3].

The synthesis of an eight-bar linkage to reach a specified set of task positions was first presented by Subbian and Flugrad (1994) [5]. They formulated design equations for a connected set of RR and RRR chains such that the resulting system could reach as many as seven task positions. This work used the triad synthesis equations studied by Lin and Erdman (1987) [6] and Chase et al.(1987) [7]. Farhang and Basu (1994) [8] developed approximate kinematic equations for the analysis and design of three input, eight-bar mechanisms driven by relatively small cranks. Mariappan and Krishnamurty (1996) [9] used exact gradient method for the synthesis of an eight-bar dwell mechanism. Recent work on the rigid body guidance of planar eight-bar linkages includes Chen and Angeles (2008) [10] where they synthesize an eight-bar linkage to reach 11 task positions, and Soh and McCarthy [11, 12] where they presented a dimensional synthesis procedure for planar eight-bars connected only by revolute joints.

Our approach is different from these previous works in that we start with a three degree-of-freedom parallel PRR-3R robot that can reach five task poses, and then add two RR constraints

to obtain an eight-bar linkage that could be driven by a prismatic base joint. This approach reduces the complexity of the design process and organizes the free parameters in a way that assists the designer. It is known that there are sixteen topologies for one degree-of-freedom eight bars linkages as shown in Figure 1, see Tsai (2001) [4]. Our 8 topologies are inversions of four of these sixteen basic chains.

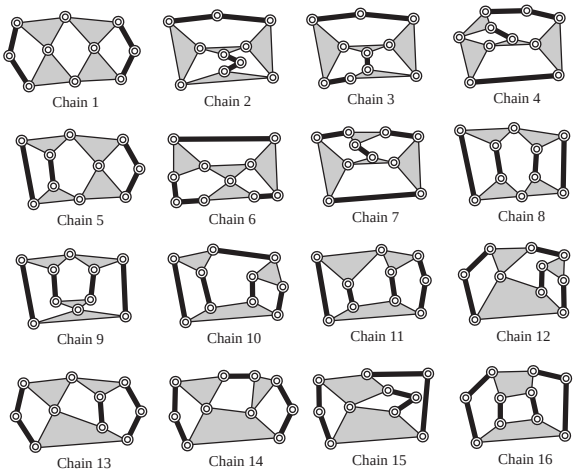

FIGURE 1. The sixteen one degree-of-freedom topologies for planar eight-bar chains.

Once an eight-bar linkage has been designed, we analyze it to determine its configuration for given values of the input slide, in order to simulate its movement. Dhingra et al. (2000) [13] present the analysis of all 16 general eight-bar linkages. For our work, we follow Wampler (2001) [14] and formulate complex number loop equations and use the Dixon determinant to eliminate joint variables, in order to analyze and simulate the movement of our eight-bar linkage.

THE KINEMATICS OF THE PLANAR PRR-3R PARALLEL ROBOT

The kinematics equations of the planar PRR-3R parallel robot equate the 3×3 homogeneous transformation $[D]$ between the end-effector and the base frame to the sequence of local coordinate transformations around the joint axes and along the links of the chain,

$$\begin{aligned}[D] =& [G_1][Z(\alpha)][X(\theta_1)][Z(\theta_2)][X(a_{23})][Z(\theta_3)][H_1], \text{and} \\ [D] =& [G_2][Z(\theta_4)][X(a_{45})][Z(\theta_5)][X(a_{56})][Z(\theta_6)][H_2]. \end{aligned} \quad (1)$$

The transformation $[Z(\theta)]$ and $[X(\alpha)]$ are the 3 x 3 homogenous matrices that represent a rotation about the z-axis by θ,

$$Z(\theta) = \begin{bmatrix} \cos\theta & -\sin\theta & 0 \\ \sin\theta & \cos\theta & 0 \\ 0 & 0 & 1 \end{bmatrix},$$

and a translation along the x-axis by α,

$$X(\alpha) = \begin{bmatrix} 1 & 0 & \alpha \\ 0 & 1 & 0 \\ 0 & 0 & 1 \end{bmatrix}. \quad (2)$$

As shown in Figure 2, the parameters θ_i define the movement at each joint and $a_{l,k}$ define the length of the links that connects between link l and k. The angle α defines the slide axes orientation with respect to the fixed frame. The transformation $[G_i]$ defines the position of the base of the chain relative to the fixed frame, and $[H_i]$ locates its task frame relative to the end-effector frame. The matrix $[D]$ defines the coordinate transformation from the world frame F to the task frame M.

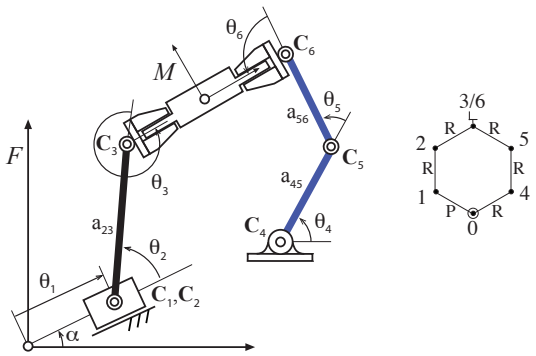

FIGURE 2. The kinematic diagram of the planar PRR-3R parallel robot. The graph of this chain has a vertex for each link and an edge for each joint. R denotes a revolute joint and P a prismatic joint.

DIMENSIONAL SYNTHESIS OF EIGHT-BAR LINKAGE

The dimensional synthesis of planar eight-bar linkages with a sliding base joint can be accomplished by constraining two RR chains to a parallel robot formed by a serial PRR and 3R chain. The selection of a parallel robot allows the designer to choose the two connections to ground and two connections on the moving workpiece, and a PRR-3R parallel robot provides the structure for prismatic actuation. Due to practical reasons, we choose not

to connect any additional links to the prismatic joint and avoid a third ground pivot.

Our dimensional synthesis process proceeds in three steps. Given five task poses, we first identify a PRR-3R parallel robot that reaches those poses. Inverse kinematics analysis of the parallel robot yields the configuration of the robot in each of the five poses. This allows us to compute the five relative poses of any pair of links in the chain.

The second step is to choose two links in the parallel robot and compute an RR chain that constrains their relative movement to that required by the five task poses. Denote the ground link as B_0, the three links of the PRR chain can be labelled as B_i, $i = 1,2,3$ and the 3R chain as B_i, $i = 4,5,6$. Because we cannot constrain two consecutive links within the PRRRRR loop and we choose not to constrain any links to the prismatic joint or to the ground, this leaves three cases: i) B_2B_4, ii) B_2B_5 and iii) B_3B_4. The introduction of this RR chain adds a link to the system that we will denote as B_7.

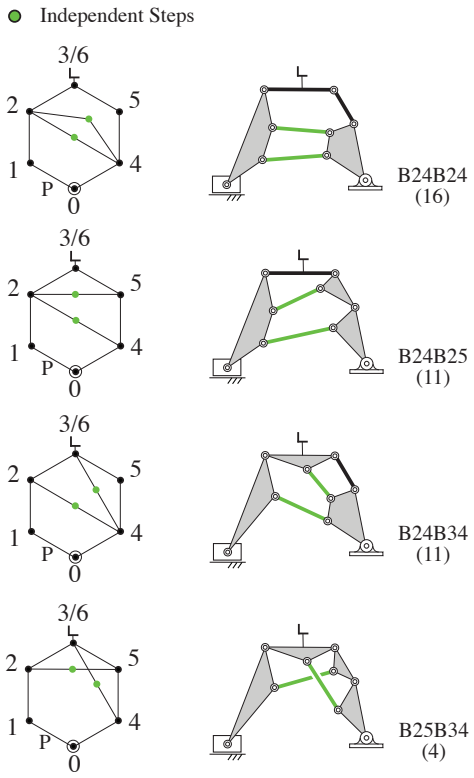

FIGURE 3. The linkage graphs show the synthesis sequence for the four planar eight-bar linkages in which the two RR chains are attached independently. The number in bracket denotes its topological chain. The graph edges denotes a revolute joint unless otherwise stated.

The third step consists of adding a second RR chain. The second RR constraint can be attached to the original parallel robot or to the newly formed link. In the first case, we found that four eight-bar structures could be designed this way. Figure 3 shows the various eight-bar structures that result from independent RR constraints to the parallel robot. We label these structures by denoting Bij as the RR constraint connecting B_i and B_j. For example, a B24B25 would have RR constraints between B_2 and B_4 as well as B_2 and B_5.

We now consider the case where an RR constraint is connected to the new link B_7. Figure 4 shows that we have four eight-bar structures that arise from such dependent attachment.

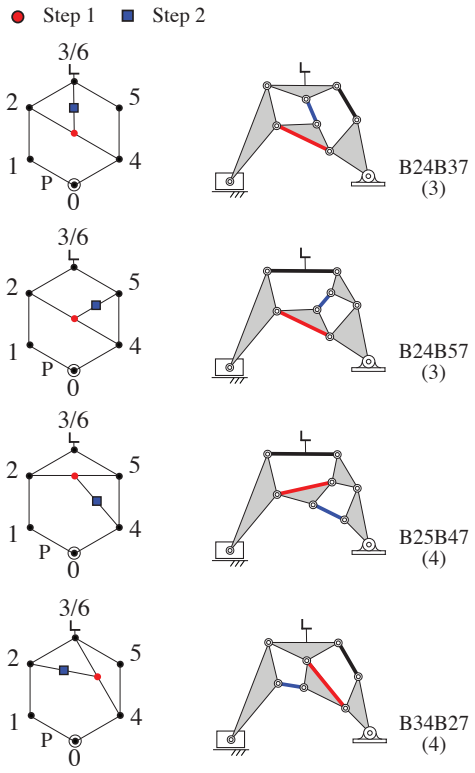

FIGURE 4. The linkage graphs show the synthesis sequence for the four planar eight-bar linkages in which the second RR chain connects to the first RR chain. The number in bracket denotes its topological chain. The graph edges denotes a revolute joint unless otherwise stated.

The Synthesis Of An RR Constraint Between Two Arbitrary Bodies

The synthesis of an RR chain to reach five task pose is well-known, and we expand the formulation by McCarthy (2010) [12] to synthesize an RR chain between two moving bodies.

Let $[B_{l,j}]$ be five poses of the lth moving link, and $[B_{k,j}]$ be the five poses of the kth moving link measured in a world frame

F, $j = 1,\ldots,5$. Let $\mathbf{g}$ be the coordinates of the R-joint attached to the lth link measured in the link frame B_l. Similarly, let $\mathbf{w}$ be the coordinates of the other R-joint measured in the link frame B_k. The five poses of these points as the two moving bodies move between the task configurations are given by

$$\mathbf{G}^j = [B_{l,j}]\mathbf{g} \quad \text{and} \quad \mathbf{W}^j = [B_{k,j}]\mathbf{w}. \tag{3}$$

Now, introduce the relative displacements

$$[R_{1j}] = [B_{l,j}][B_{l,1}]^{-1} \quad \text{and} \quad [S_{1j}] = [B_{k,j}][B_{k,1}]^{-1}, \tag{4}$$

so these equations become

$$\mathbf{G}^j = [R_{1j}]\mathbf{G}^1 \quad \text{and} \quad \mathbf{W}^j = [S_{1j}]\mathbf{W}^1, \tag{5}$$

where $[R_{11}] = [S_{11}] = [I]$ are the identity transformations.

The point $\mathbf{G}^j$ and $\mathbf{W}^j$ define the ends of a rigid link of length a, therefore we have the constraint equations as defined by the dot product,

$$([S_{1j}]\mathbf{W}^1 - [R_{1j}]\mathbf{G}^1) \cdot ([S_{1j}]\mathbf{W}^1 - [R_{1j}]\mathbf{G}^1) = a^2. \tag{6}$$

These five equations can be solved to determine the five design parameters of the RR constraint, $\mathbf{G}^1 = (u,v,1)^T$, $\mathbf{W}^1 = (x,y,1)^T$ and a. We will refer to these equations as the *synthesis equations* for the RR link. To solve the synthesis equations, it is convenient to introduce the displacements

$$[D_{1j}] = [R_{1j}]^{-1}[S_{1j}] = [B_{l,1}][B_{l,j}]^{-1}[B_{k,j}][B_{k,1}]^{-1}, \tag{7}$$

so these equations become

$$([D_{1j}]\mathbf{W}^1 - \mathbf{G}^1) \cdot ([D_{1j}]\mathbf{W}^1 - \mathbf{G}^1) = a^2. \tag{8}$$

Subtract the first of these equations from the remaining to cancel a^2 and the square terms in the variables u,v and x,y. The resulting four bilinear equations can be solved algebraically (see McCarthy (2010) [12]), or numerically using something equivalent to *Mathematica's* `Nsolve` function to obtain the desired pivots.

EXAMPLE SYNTHESIS OF A TRANSFORMATIVE WHEELCHAIR

The goal here is to design a multi-functional wheelchair that could transform itself between a self-propelled wheelchair and a walking guide. This not only provides outpatients the ability to perform rehabilitation exercise on their own by transforming itself to a walking-aid apparatus but also as a means of transportation during their recovery period. It also provides the structure for robotic systems to be fitted onto the wheel chair to monitor their recovery status and to give them professional guidance. The benefit of such transformative wheelchair is that it eliminates the need for the user to carry an additional rehabilitative device around. We choose to use a cantilever frame (see Cooper (1995) [15]) and attached an eight-bar linkage as its arm and armrest to achieve this. This is an improvement to the design as presented by Soh etal. (2012) [16].

TABLE 1. Five task poses for the end-effector of the parallel robot that transform between a wheelchair and a walking guide.

Task	*Pose* $(\theta(^\circ), x(in), y(in))$
1	$(0, 11, 7.5)$
2	$(-10.1, 11, 8.38)$
3	$(-20.6, 11, 9.26)$
4	$(-32.0, 11, 10.15)$
5	$(-44.9, 11, 11.03)$

The task poses that define such movement are listed in Table 1 and as shown at the bottom right image of Figure 5. These poses define the discrete handle position of the walking guide. Note that the poses of the arm rest as denoted by the rectangle, are to cater to patients of varying heights. In the following, we design a B24B24 linkage to achieve such task.

We select the link dimensions of the parallel robot to be as shown in Table 2 (see Figure 2 for the notations). Thus, for a given set of five task poses $[M_j]$, $j = 1,\ldots,5$, we solve the inverse kinematics equations to determine the associated joint parameters vectors $\mathbf{q}_i = (\theta_{1j}, \theta_{2j}, \theta_{3j}, \theta_{4j}, \theta_{5j}, \theta_{6j})$, $j = 1,\ldots,5$. The coordinates of the five R joints in each of the five configurations are denoted by $\mathbf{C}_{2j}$, $\mathbf{C}_{3j}$, $\mathbf{C}_{4j}$, $\mathbf{C}_{5j}$, and $\mathbf{C}_{6j}$, $j = 1,\ldots,5$.

Link	$[G_1]$	$\alpha(^\circ)$	$a_{23}(in)$	$[H_1]$
PRR	$(0^\circ, 19.1, 0)$	180	11.04	$(0^\circ, 0, 0)$
Link	$[G_2]$	$a_{45}(in)$	$a_{56}(in)$	$[H_1]$
3R	$(180^\circ, 0, 0)$	7.9	13.23	$(0^\circ, -14, 0)$

TABLE 2. The chosen parameters of the parallel robot.

	$\mathbf{G}^1$	$\mathbf{W}^1$
1	$(5.61,-1.50,1)$	$(7.04,-3.53,1)$
2	$(1.92,0.96,1)$	$(13.02,3.83,1)$
3	*Complex*	*Solution*
4	*Complex*	*Solution*

TABLE 3. Solutions for both $\mathbf{G}_1^1\mathbf{W}_1^1$ and $\mathbf{G}_2^1\mathbf{W}_2^1$.

For the five configurations, we can identify the poses of each of the six links of the parallel robot using the coordinate transformations $[B] = [A(\theta), \mathbf{C}]$, in which $\mathbf{C}_i$ is the coordinates of the origin of the link frames, and A is a rotation matrix of angle θ relative to the ground frame F. Using this convention and ignoring the sliding first link, the poses of the second to sixth links are given by

$$\begin{aligned}
[B_{2j}] &= [A(\alpha+\theta_{2j}), \mathbf{C}_{2j}],\\
[B_{3j}] &= [A(\alpha+\theta_{2j}+\theta_{3j}), \mathbf{C}_{3j}],\\
[B_{4j}] &= [A(\theta_{4j}), \mathbf{C}_{4j}],\\
[B_{5j}] &= [A(\theta_{4j}+\theta_{5j}), \mathbf{C}_{5j}],\\
\text{and } [B_{6j}] &= [A(\theta_{4j}+\theta_{5j}+\theta_{6j}), \mathbf{C}_{6j}], \quad j = 1,\ldots,5. \qquad (9)
\end{aligned}$$

The 25 coordinate transformations, $[B_{ij}]$, form the requirements used to synthesize two RR chains that constrain the movement of the chain to pass through the given task poses. We compute the RR chain $\mathbf{G}_1^1\mathbf{W}_1^1$ and $\mathbf{G}_2^1\mathbf{W}_2^1$ using Eq (8) with $[D_{1j}] = [B_{2,1}][B_{2,j}]^{-1}[B_{4,j}][B_{4,1}]^{-1}$ to constraint between B_2 and B_4. Since we are constraining between the same bodies twice, the solutions are listed in Table 3.

A schematic of the resulting planar eight bar linkage at each of the five poses is shown by the image sequence labelled 1-5 in Figure 5.

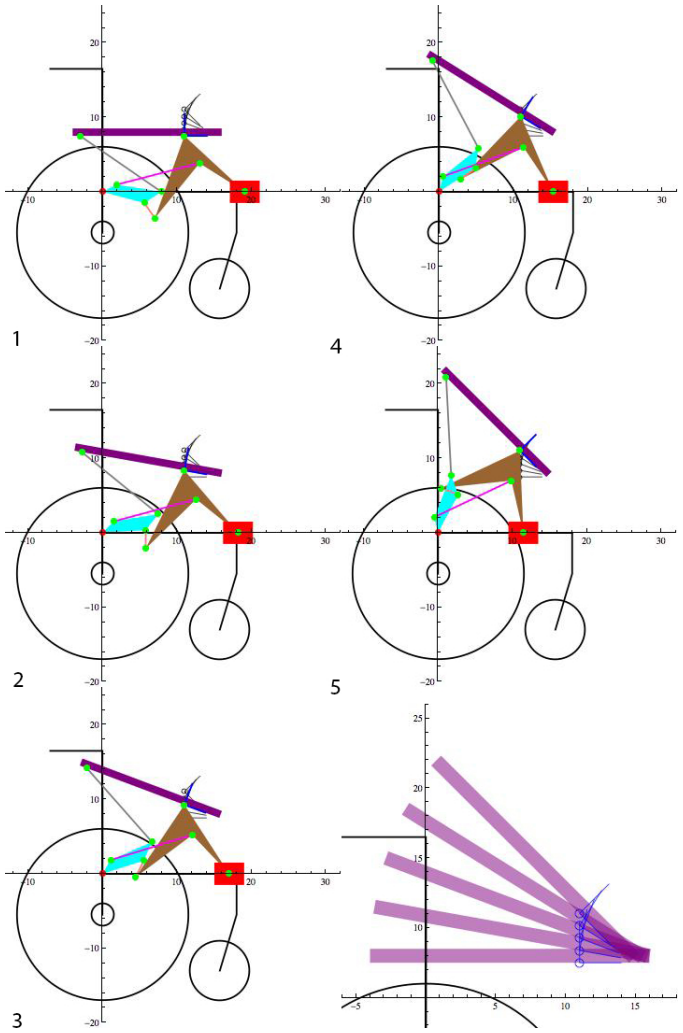

FIGURE 5. The image sequence for the B24B24 planar eight-bar linkage reaching a set of five task poses. The bottom right image shows a close up view of the poses.

ANALYSIS OF PLANAR EIGHT-BAR LINKAGES: B24B24

To analyze the planar B24B24 eight-bar linkage, we use complex number coordinates and the Dixon determinant as presented by Wampler (2001) [14]. This approach can be generalized for any planar eight-bar linkage.

The Complex Loop Equations

Consider the B24B24 linkage with links and joint parameters θ_i as shown in Figure 6. Introduced a coordinate frame F such that its origin coincides with the configuration of $\mathbf{C}_1$ at its first pose and with its x-axis is directed towards $\mathbf{C}_3$. Using the notation in Figure 6, we formulate the complex loop equations formed by loop $\mathbf{OC}_1\mathbf{W}_1\mathbf{G}_1\mathbf{C}_3$, $\mathbf{OC}_1\mathbf{W}_2\mathbf{G}_2\mathbf{C}_3$ and $\mathbf{OC}_1\mathbf{C}_2\mathbf{C}_5\mathbf{C}_4\mathbf{C}_3$, that is,

$$\begin{aligned}
f_1: &\quad \Theta_0 e^{i\alpha} + b_1\Theta_1 e^{-i\gamma} - l_5\Theta_5 - b_2\Theta_3 e^{i\eta} - l_0 = 0,\\
f_2: &\quad \Theta_0 e^{i\alpha} + b_3\Theta_1 e^{-i\beta} - l_6\Theta_6 - b_4\Theta_3 e^{i\varepsilon} - l_0 = 0,\\
f_3: &\quad \Theta_0 e^{i\alpha} + l_1\Theta_1 + l_2\Theta_2 - l_3\Theta_3 - l_4\Theta_4 - l_0 = 0. \qquad (10)
\end{aligned}$$

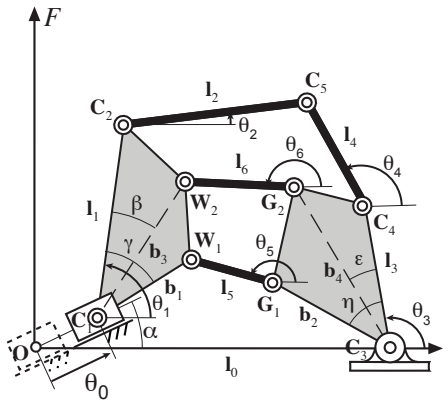

FIGURE 6. This shows our conventions for the analysis of the B24B24 linkage.

The complex conjugate of these equations yields

$$\begin{aligned}
f_1^\star: &\quad \Theta_0 e^{-i\alpha} + b_1\Theta_1^{-1}e^{i\gamma} - l_5\Theta_5^{-1} - b_2\Theta_3^{-1}e^{-i\eta} - l_0 = 0,\\
f_2^\star: &\quad \Theta_0 e^{-i\alpha} + b_3\Theta_1^{-1}e^{i\beta} - l_6\Theta_6^{-1} - b_4\Theta_3^{-1}e^{-i\varepsilon} - l_0 = 0,\\
f_3^\star: &\quad \Theta_0 e^{-i\alpha} + l_1\Theta_1^{-1} + l_2\Theta_2^{-1} - l_3\Theta_3^{-1} - l_4\Theta_4^{-1} - l_0 = 0.
\end{aligned} \tag{11}$$

We solve these six equations for Θ_j, $j = 1,2,3,4,5,6$ using the Dixon determinant.

The Dixon Determinant

We suppress Θ_2, so we have six complex equations in the five variables Θ_1, Θ_3, Θ_4, Θ_5 and Θ_6. We formulate the Dixon determinant by inserting each of the six functions f_1, f_1^*, f_2, f_2^*, f_3, f_3^* as the first row, and then sequentially replacing the five variables by α_i in the remaining rows, to obtain,
$\Delta(f_1, f_1^*, f_2, f_2^*, f_3, f_3^*) =$

$$\begin{vmatrix}
f_1(\Theta_1,\Theta_3,\Theta_4,\Theta_5,\Theta_6) & \dots & f_3^*(\Theta_1,\Theta_3,\Theta_4,\Theta_5,\Theta_6)\\
f_1(\alpha_1,\Theta_3,\Theta_4,\Theta_5,\Theta_6) & \dots & f_3^*(\alpha_1,\Theta_3,\Theta_4,\Theta_5,\Theta_6)\\
\vdots & & \vdots\\
f_1(\alpha_1,\alpha_3,\alpha_4,\alpha_5,\alpha_6) & \dots & f_3^*(\alpha_1,\alpha_3,\alpha_4,\alpha_5,\alpha_6)
\end{vmatrix}. \tag{12}$$

This determinant is zero when Θ_j, $j = 1,\dots,6$ satisfy the loop equations, because the elements of the first row become zero.

Now row reduce Δ by subtracting the second row from the first row, then the third from the second, fourth from the third, and the fifth from the fourth, to obtain,

$$\begin{vmatrix}
c_{11}(\Theta_1-\alpha_1) & \dots & c_{31}^*(\Theta_1^{-1}-\alpha_1^{-1})\\
c_{13}(\Theta_3-\alpha_3) & \dots & c_{33}^*(\Theta_3^{-1}-\alpha_3^{-1})\\
\vdots & & \vdots\\
f_1(\alpha_1,\alpha_3,\alpha_4,\alpha_5,\alpha_6) & \dots & f_3^\star(\alpha_1,\alpha_3,\alpha_4,\alpha_5,\alpha_6)
\end{vmatrix}. \tag{13}$$

This determinant contains extraneous roots of the form $\Theta_j = \alpha_j$ and can be removed by factoring out $(\Theta_j^{-1} - \alpha_j^{-1})$. We substitute $\Theta_j - \alpha_j = -\Theta_j\alpha_j(\Theta_j^{-1} - \alpha_j^{-1})$, to obtain,

$$\delta = \frac{\Delta(f_1, f_1^*, f_2, f_2^*, f_3, f_3^*)}{\prod_{i=1,3,4,5,6}(\Theta_i^{-1} - \alpha_i^{-1})}. \tag{14}$$

This determinant expands to form the Dixon polynomial

$$\delta = \mathbf{a}[W]\mathbf{t} = 0. \tag{15}$$

$\mathbf{a} = \{\mathbf{a}_1\ \mathbf{a}_2\}$ is a row vector of monomials such that $\mathbf{a}_1$ is any combinations $\alpha_i\alpha_j$ of the variables $(\alpha_1,\alpha_3,\alpha_4,\alpha_5,\alpha_6)$, and $\mathbf{a}_2$ is its complement $\alpha_k\alpha_l\alpha_m$ as follows:

$$\mathbf{a}_1^T = \begin{Bmatrix}
\alpha_1\alpha_3\\ \alpha_1\alpha_4\\ \alpha_1\alpha_5\\ \alpha_1\alpha_6\\ \alpha_3\alpha_4\\ \alpha_3\alpha_5\\ \alpha_3\alpha_6\\ \alpha_4\alpha_5\\ \alpha_4\alpha_6\\ \alpha_5\alpha_6
\end{Bmatrix}\ \mathbf{a}_2^T = \begin{Bmatrix}
\alpha_4\alpha_5\alpha_6\\ \alpha_3\alpha_5\alpha_6\\ \alpha_3\alpha_4\alpha_6\\ \alpha_3\alpha_4\alpha_5\\ \alpha_1\alpha_5\alpha_6\\ \alpha_1\alpha_4\alpha_6\\ \alpha_1\alpha_4\alpha_5\\ \alpha_1\alpha_3\alpha_6\\ \alpha_1\alpha_3\alpha_5\\ \alpha_1\alpha_3\alpha_4
\end{Bmatrix}. \tag{16}$$

Similarly for $\mathbf{t} = \begin{Bmatrix}\mathbf{t}_1\\ \mathbf{t}_2\end{Bmatrix}$ we have the following column vectors of monomials:

$$\mathbf{t}_1 = \begin{Bmatrix}
\Theta_1\Theta_3\\ \Theta_1\Theta_4\\ \Theta_1\Theta_5\\ \Theta_1\Theta_6\\ \Theta_3\Theta_4\\ \Theta_3\Theta_5\\ \Theta_3\Theta_6\\ \Theta_4\Theta_5\\ \Theta_4\Theta_6\\ \Theta_5\Theta_6
\end{Bmatrix}\ \mathbf{t}_2 = \begin{Bmatrix}
\Theta_4\Theta_5\Theta_6\\ \Theta_3\Theta_5\Theta_6\\ \Theta_3\Theta_4\Theta_6\\ \Theta_3\Theta_4\Theta_5\\ \Theta_1\Theta_5\Theta_6\\ \Theta_1\Theta_4\Theta_6\\ \Theta_1\Theta_4\Theta_5\\ \Theta_1\Theta_3\Theta_6\\ \Theta_1\Theta_3\Theta_5\\ \Theta_1\Theta_3\Theta_4
\end{Bmatrix}. \tag{17}$$

The matrix [W] can be rewritten in a way such that matrices D_1 and D_2 are diagonal, and the elements of A obey the relation $a_{ij} = a^*_{ji}$, that is,

$$\{\mathbf{a}_1\ \mathbf{a}_2\}\begin{bmatrix} D_1 x + D_2 & A^T \\ A & D_1^* x^{-1} + D_2^* \end{bmatrix}\begin{Bmatrix}\mathbf{t}_1 \\ \mathbf{t}_2\end{Bmatrix} = 0. \tag{18}$$

Solving the loop equations

A set of values Θ_j that satisfy the loop equations (10) and (11) will also yield $\delta = 0$, which will be true for arbitrary values of the auxiliary variables α_j. Thus solutions for these loop equations must also satisfy the matrix equation,

$$[W]\mathbf{t} = 0. \tag{19}$$

The matrix W is a square, therefore this equation has solutions only if $\det[W] = 0$. Expanding this determinant we obtain a polynomial in $x = \Theta_2$. The structure $[W]$ yields,

$$\begin{aligned}[W]\mathbf{t} &= \left[\begin{pmatrix} D_1 & 0 \\ A & D_2^* \end{pmatrix} x - \begin{pmatrix} -D_2 & -A^T \\ 0 & -D_1^* \end{pmatrix}\right]\begin{Bmatrix}\mathbf{t}_1 \\ \mathbf{t}_2\end{Bmatrix} \\ &= [Mx - N]\mathbf{t} = 0.\end{aligned} \tag{20}$$

Notice that the values of x that result in $\det[W] = 0$ are also the eigenvalues of the characteristic polynomial $p(x) = det(Mx - N)$ of the generalized eigenvalue problem

$$N\mathbf{t} = xM\mathbf{t}. \tag{21}$$

Each value of $x = \Theta_2$ has an associated eigenvector $\mathbf{t}$ which yields the values of the remaining joint angles $\Theta_j, j = 1,3,4,5,6$.

It is useful to notice that each eigenvector $\mathbf{t} = (t_1, \ldots, t_{20})^T$ is defined up to a constant multiple, say μ. Therefore it is convenient to determine the values of Θ_j, by computing the ratios,

$$\Theta_1 = \tfrac{t_{20}}{t_5} = \tfrac{\mu\Theta_1\Theta_3\Theta_4}{\mu\Theta_3\Theta_4},\ \Theta_3 = \tfrac{t_{20}}{t_2} = \tfrac{\mu\Theta_1\Theta_3\Theta_4}{\mu\Theta_1\Theta_4},\ \Theta_4 = \tfrac{t_{20}}{t_1} = \tfrac{\mu\Theta_1\Theta_3\Theta_4}{\mu\Theta_1\Theta_3},$$

$$\Theta_5 = \tfrac{t_{19}}{t_1} = \tfrac{\mu\Theta_1\Theta_3\Theta_5}{\mu\Theta_1\Theta_3},\ \Theta_6 = \tfrac{t_{18}}{t_1} = \tfrac{\mu\Theta_1\Theta_3\Theta_6}{\mu\Theta_1\Theta_3}. \tag{22}$$

Sorting the Assemblies

The closed form solution above would yield as many as 20 configurations for each input slide. Therefore, to analyze the B24B24 eight-bar linkage for a sequence of input slide Θ_0, we need to sort each of these joints angles into their respective assemblies. This can be done using Newton's method.

First, compute the derivative of the loop equations (10) and (11) to obtain

$$\begin{aligned}
\nabla f_1 &: \quad \dot\Theta_0 e^{i\alpha} + b_1\dot\Theta_1 e^{-i\gamma} - l_5\dot\Theta_5 - b_2\dot\Theta_3 e^{i\eta} = 0,\\
\nabla f_2 &: \quad \dot\Theta_0 e^{i\alpha} + b_3\dot\Theta_1 e^{-i\beta} - l_6\dot\Theta_6 - b_4\dot\Theta_3 e^{i\varepsilon} = 0,\\
\nabla f_3 &: \quad \dot\Theta_0 e^{i\alpha} + l_1\dot\Theta_1 + l_2\dot\Theta_2 - l_3\dot\Theta_3 - l_4\dot\Theta_4 = 0,\\
\nabla f_1^\star &: \quad \dot\Theta_0 e^{-i\alpha} + b_1\dot\Theta_1\Theta_1^{-2} e^{i\gamma} - l_5\dot\Theta_5\Theta_5^{-2} - b_2\dot\Theta_3\Theta_3^{-2} e^{-i\eta} = 0,\\
\nabla f_2^\star &: \quad \dot\Theta_0 e^{-i\alpha} + b_3\dot\Theta_1\Theta_1^{-2} e^{i\beta} - l_6\dot\Theta_6\Theta_6^{-2} - b_4\dot\Theta_3\Theta_3^{-2} e^{-i\varepsilon} = 0,\\
\nabla f_3^\star &: \quad \dot\Theta_0 e^{-i\alpha} + l_1\dot\Theta_1\Theta_1^{-2} + l_2\dot\Theta_2\Theta_2^{-2} - l_3\dot\Theta_3\Theta_3^{-2} - l_4\dot\Theta_4\Theta_4^{-2} = 0.
\end{aligned} \tag{23}$$

Now, factor out the derivative vector $\dot{\vec\Theta} = (\Theta_1, \Theta_2, \Theta_3, \Theta_4, \Theta_5, \Theta_6)$ to obtain the Jacobian matrix,

$$[\nabla\mathscr{F}(\vec\Theta)]\dot{\vec\Theta} = 0. \tag{24}$$

To sort the roots among the various assemblies of the eight-bar linkage, we approximate the complex loop equations using the Jacobian, $\nabla\mathscr{F}(\vec\Theta)$ and obtain

$$[\nabla\mathscr{F}(\vec\Theta^k)](\vec\Psi - \vec\Theta^k) = 0. \tag{25}$$

$\vec\Psi$ approximates the value of $\vec\Theta^{k+1}$ associated with the input slide Θ_0^{k+1} and is near to the assembly defined by $\vec\Theta^k$. The task now is to identify which root $\vec\Theta^{k+1}$ is closest to $\vec\Psi$ on the ith circuit to match the assemblies.

Numerical Example

To analyze the B24B24 planar eight-bar linkage that results, we first determine the range of input slide θ_0 by computing the inverse kinematics of the PRR-3R parallel robot at each of the task pose M. This yields five input slide parameters, which we interpolate between them to obtain 24 input slide parameters for this analysis. Table 4 shows the solutions for each of the 24 input slide θ_0 that correspond to the assembly configuration associated with the first pose after our sorting process.

CONCLUSION

This paper presents a dimensional synthesis procedure for planar eight-bar linkages by constraining a parallel robot with a prismatic base. This procedure yields 8 different types of eight-bar structures. The resulting linkage provides designers the capability to use linear actuators to drive directly at its prismatic base

	$\theta_0(in)$	$\theta_1(^\circ)$	$\theta_2(^\circ)$	$\theta_3(^\circ)$	$\theta_4(^\circ)$	$\theta_5(^\circ)$	$\theta_6(^\circ)$
1	0.00	-42.80	0.00	180.00	-34.53	125.10	-165.50
2	0.18	-44.18	-2.38	-174.84	-34.87	115.00	-165.62
3	0.37	-45.53	-4.48	-170.79	-35.63	107.30	-165.55
4	0.55	-46.84	-6.45	-167.34	-36.62	100.80	-165.39
5	0.73	-48.13	-8.32	-164.28	-37.78	95.06	-165.17
6	0.91	-49.39	-10.14	-161.50	-39.06	89.91	-164.92
7	0.91	-49.39	-10.14	-161.50	-39.06	89.91	-164.92
8	1.15	-50.98	-12.39	-158.24	-40.83	83.89	-164.56
9	1.38	-52.53	-14.57	-155.23	-42.70	78.38	-164.17
10	1.62	-54.05	-16.66	-152.44	-44.63	73.26	-163.77
11	1.86	-55.55	-18.68	-149.81	-46.60	68.45	-163.36
12	2.09	-57.02	-20.61	-147.32	-48.58	63.90	-162.95
13	2.09	-57.02	-20.61	-147.32	-48.58	63.90	-162.95
14	2.42	-59.06	-23.21	-143.97	-51.40	57.80	-162.36
15	2.76	-61.06	-25.65	-140.81	-54.18	52.05	-161.77
16	3.09	-63.03	-27.92	-137.80	-56.92	46.57	-161.20
17	3.43	-64.95	-30.03	-134.90	-59.60	41.33	-160.63
18	3.76	-66.85	-32.01	-132.08	-62.22	36.33	-160.07
19	3.76	-66.85	-32.01	-132.08	-62.22	36.33	-160.07
20	4.54	-71.05	-36.40	-125.35	-68.43	26.63	-158.88
21	5.32	-75.56	-38.72	-120.52	-72.83	12.01	-157.59
22	6.10	-79.66	-41.41	-114.62	-77.93	1.56	-156.52
23	6.87	-83.71	-43.44	-108.83	-82.62	-9.34	-155.52
24	7.65	-87.68	-44.91	-102.91	-87.06	-20.62	-154.59

TABLE 4. Analysis solution for each input slide θ_0 that correspond to the assembly configuration associated with the first pose.

joint. The synthesis and analysis procedure are demonstrated by an example design of a B24B24 linkage for use as a transformative linkage for a multipurpose wheelchair. The result shows the benefit of such design process in using free parameters of the backbone chain to define the location of the ground pivots as well as the connections of the moving workpiece for which a 4R and planar six-bar linkage cannot provide.

ACKNOWLEDGEMENT

The authors gratefully acknowledge the financial support of ZJU-SUTD Research Collaboration Grant (Project SUTD-ZJU/PILOT/02/2011) and SUTD-MIT International Design Center (Grant No. IDG11200103 and IDD11200106).

REFERENCES

[1] D. H. Myszka and A. P. Murray, 2010, "Pole arrangements that introduce prismatic joints into the design space of four- and five-position rigid-body synthesis", *Mechanism and Machine Theory*, 45(9):13141325.

[2] G. A. Gazonas, S. B. Segletes, V. M. Boyle and S. R. Stegall, 1996, "Oblique Impact Modeling of Fuzes", *International Journal of Impact Engineering*, 18(4):435-457.

[3] T. Koetsier, 1983, "A Contribution to the History of Kinematics-I," *Mechanism and Machine Theory*, 18(1):37-42.

[4] L. W. Tsai, 2001, *Enumeration of Kinematic Structures According to Function*, Florida, CRC Press LLC.

[5] T. Subbian, and D. R. Flugrad, 1994, "6 and 7 Position Triad Synthesis using Continuation Methods," *Journal of Mechanical Design*, 116(2):660-665.

[6] C. S. Lin, and A. G. Erdman, 1987, "Dimensional Synthesis of Planar Triads for Six Positions," *Mechanism and Machine Theory*, 22:411-419.

[7] T. R. Chase, A. G. Erdman, and D. R. Riley, 1987, "Triad Synthesis for up to 5 Design Positions with Applications to the Design of Arbitrary Planar Mechanisms," *ASME Journal of Mechanisms, Transmissions and Automation in Design*, 109(4):426-434.

[8] K. Farhang and P. S. Basu, 1994, "Kinematic Analysis and Synthesis of Three-Input, Eight-Bar Mechanisms Driven by Relatively Small Cranks," *Journal of Mechanical Design*, 116(3):930-936.

[9] J. Mariappan and S. Krishnamurty, 1994, "A Generalized Exact Gradient Method for Mechanism Synthesis," *Mechanism and Machine Theory*, 31(4):413-421.

[10] C. Chen, and J. Angeles, 2008, "A novel family of linkages for advanced motion synthesis," *Mechanism and Machine Theory*, 43(7):882-890.

[11] G. S. Soh and J. M. McCarthy, 2007,"Synthesis of Mechanically Constrained Planar 2-RRR Planar Parallel Robots," *Proceedings of the 2007 IFToMM World Congress*, Besanon, France

[12] J. M. McCarthy and G.S. Soh, 2010, *Geometric Design of Linkages, Second Edition*, Interdisciplinary Applied Mathematics, Springer Verlag, New York.

[13] A. K. Dhingra, A. N. Almadi, and D. Kohli, 2000, "Closed-form displacement analysis of 8, 9, and 10-link mechanisms, Part I: 8-link 1-DOF mechanisms," *Mechanism and Machine Theory*, 35:821-850.

[14] C. W. Wampler, 2001, "Solving the Kinematics of Planar Mechanisms by Dixon Determinant and a Complex Plane Formulation", *ASME Journal of Mechanical Design*, 123(3), pp. 382-387.

[15] R. A. Cooper, 1995, *Rehabilitation Engineering Applied to Mobility and Manipulation*, Institute of Physics Publishing, Bristol, UK.

[16] G. S. Soh, F. Ying and J. M. McCarthy, 2012,"Dimensional Synthesis of Planar Six-Bar Linkages by Mechanically Constrain a PRR Serial Chain," *Proceedings of the ASME International Design Engineering Technical Conference*, Chicago, USA